Received: 4 May 2020 | Revised: 23 June 2020 | Accepted: 11 July 2020

DOI: 10.1002/ardp.202000140

FULL PAPER

DPhG ARCH PHARM Archiv der Pharmazie

Novel thiazole–pyrazolone hybrids as potent ACE inhibitors and their cardioprotective effect on isoproterenol-induced myocardial infarction

Hongwen You[1] | Xinyou Su[2] | Guoying Su[3]

[1]Department of Cardiology, Shandong Provincial Hospital Affiliated to Shandong First Medical University, Jinan, Shandong, China

[2]Department of Oncology, Jinan Central Hospital, Cheeloo College of Medicine, Shandong University, Jinan, Shandong, China

[3]Department of Cardiology, Jinan Central Hospital, Cheeloo College of Medicine, Shandong University, Jinan, Shandong, China

Correspondence
Guoying Su, Department of Cardiology, Jinan Central Hospital, Cheeloo College of Medicine, Shandong University, Jinan, 250013 Shandong, China.
Email: suguoyingxn@sina.com

Abstract

A facile synthesis of a group of novel thiazole–pyrazolone hybrids and their investigation for angiotensin-converting enzyme (ACE) inhibition are reported in this study. These compounds were synthesized using a well-known approach, based on the condensation of ethyl acetoacetate with thiazolylhydrazines, and characterized by various spectroscopic and analytical techniques. The entire set of compounds displayed a moderate-to-excellent inhibitory activity against ACE. In particular, compound **4i** was found to be the most potent ACE inhibitor and was further studied for cardioprotective effects against isoproterenol (ISO)-induced myocardial infarction (MI) in rats. Compound **4i** improved the cardiac function and prevented cardiac injury induced by ISO in Sprague Dawley rats. The levels of oxidative stress and proinflammatory cytokines were also restored to near normal by **4i** as compared with the ISO group. In the Western blot analysis, compound **4i** prevented mitochondrial apoptosis after MI by downregulating the expression of cleaved caspase-3 and Bax, with the upregulation of Bcl-2, as compared with the ISO group.

KEYWORDS

ACE, inflammation, myocardial infarction, oxidative stress, thiazole

1 | INTRODUCTION

Cardiovascular diseases (CVDs) are ranked after cancer as a major cause of morbidity and mortality across both developed and developing nations.[1] Myocardial infarction (MI) is the most common cause of death among patients with CVDs.[2] According to an estimate, in the past 30 years, the CVD risk has risen significantly in China due to adapting of western lifestyle, aging population, and increased urbanization.[3] In 2014, approximately 290 million patients with CVD were reported in China, among which 2.5 million were MI patients.[4] However, numerous clinical agents are currently in practice to curb the menace of MI, but no single agent has been proven effective in its management. Therefore, patients with acute MI could be managed alone or in a combination of modalities including direct angioplasty or fibrinolysis, aspirin, angiotensin-converting enzyme (ACE) inhibitors, beta blockers, and nitrates.[5,6] Particularly, the ACE inhibitor in a meta-analysis was found to improve the survival rate and disease progression if administered within 3–16 days of infarction.[7,8] The ACE is an enzyme causing the endogenous conversion of angiotensin (AT) I to AT II. This conversion triggers vasoconstriction, which results in increased blood pressure. Therefore, to meet the normal blood demand, the heart has to work more, which further weakens the cardiac muscles. Thus, drugs that prevent the action of ACE (ACE inhibitors) reduce vasoconstriction by preventing conversion to AT II and exert beneficial effect against MI.[9–12]

Heterocyclic molecules are well known for their importance as medicinal agents providing benefit against many diseases and pathological conditions.[13] Pyrazole is a five-membered heterocyclic ring responsible for a variety of pharmacological effects such as antibacterial,[14–16] antifungal,[17–19] antiviral,[20–22] and anticancer effects.[23,24] However, thiazole is another five-membered ring system that possesses numerous medicinal properties.[25] In a

pioneering study by Jiang et al.,[26] numerous thiazole-bearing pyrazoles were synthesized as a potent inhibitor of ACE inhibitors. Prompted by the above aspects, in the present manuscript, we intend to synthesize novel thiazole-bearing pyrazole derivatives as potent inhibitors of ACE, with a cardioprotective effect on isoproterenol (ISO)-induced MI in rats.

2 | RESULTS AND DISCUSSION

The compounds bearing various substituents were synthesized via a facile procedure, as shown in Scheme 1. Initially, the synthesis was started with the development of compounds **2a–j** by brominating the corresponding acetophenone derivatives **1a–j**. Compounds **2a–j** further underwent the cyclocondensation reaction with thiosemicarbazide to yield thiazolylhydrazines **3a–j**. The synthesis of target compounds **4a–j** was achieved via refluxing compounds **3a–j** with ethyl acetoacetate in the presence of dimethylformamide (DMF).[27] All synthesized compounds were characterized by different spectroscopic methods such as Fourier-transform infrared (FTIR) spectroscopy, ^{1}H nuclear magnetic resonance (NMR), ^{13}C NMR, and mass and elemental analysis. The title compounds showed characteristic peaks for each functional group in FTIR spectra, such as one absorption band at 3,385–3,391 cm^{-1} due to the presence of the N–H group in the pyrazole ring. Absorption bands at 3,081–3,087 cm^{-1} were attributed to the stretching vibration of the C–H group of the phenyl ring. Another FTIR peak at 2,952–2,959 cm^{-1} showed the presence of the CH_3 group in the pyrazole ring. The absorption band appearing at 1,682–1,689 cm^{-1} suggested the presence of C═N group of the thiazole ring. However, the stretching vibration at 1,709–1,719 cm^{-1} was found due to C═O group in the pyrazole ring. The thiazole C–S group appeared at 634–639 cm^{-1}. Another aromatic OH group appeared at 3,427 cm^{-1}. The stretching vibration of the fluoro group linked to the phenyl ring appeared at 1,538 cm^{-1}. The aromatic chloro group appeared at 787 cm^{-1}. All synthesized compounds showed characteristic peaks for each proton in ^{1}H NMR spectra. For instance, compounds of series **4a–j** showed a doublet peak corresponding to the protons of aromatic ring, which appeared at 7.62–7.87 ppm. The C–H of the thiazole group appeared as a singlet at the chemical shift range of 7.18–7.41 ppm. Furthermore, C–H protons of pyrazole moiety appeared at 5.64–5.67 ppm as a singlet. The N–H group of protons of pyrazole moiety appeared as a singlet in the chemical shift range of 3.96–3.99 ppm. The proton in the CH_3 group linked with pyrazole moiety appeared as a singlet at the chemical shift range of 2.24–2.36 ppm. In ^{13}C NMR spectra, the entire set of compounds showed a chemical shift in the range of 173.2–105.1 ppm due to the thiazole carbon atom. The pyrazole carbon was found at 165.8–94.1 ppm. The chemical shift range of 13.9–13.4 ppm was attributed to the methyl group at the pyrazole ring. Moreover, the aromatic carbon of target compounds appeared at 133.4–127.6 ppm. Finally, the mass and elemental analysis of all the synthesized compounds **4a–j** was also performed to ascertain their structure.

The compounds were obtained in excellent yield and purity, as determined by various spectroscopic and analytical procedures. The inhibitory activity of these compounds at 1.0-μM concentration of test and standard compound (lisinopril) was determined against ACE, and the results are presented in Table 1. It has been found that the entire set of the synthesized compounds showed a moderate-to-considerable ACE inhibition, ranging from 43% to 95%. It was observed that compound **4a** with no substitution on the phenyl ring showed the least activity (43%) among the tested derivatives. The activity was significantly improved in the case of compound **4b** upon insertion of the substituent (*p*-hydroxy, 67%). However, the activity dropped markedly after replacing hydroxy with methyl (**4c**). A mild increase in the activity was reported by compound **4d** upon the introduction of *para*-methoxy. Moreover, the percentage of inhibition was found to be increased upon the insertion of an electron-withdrawing group,

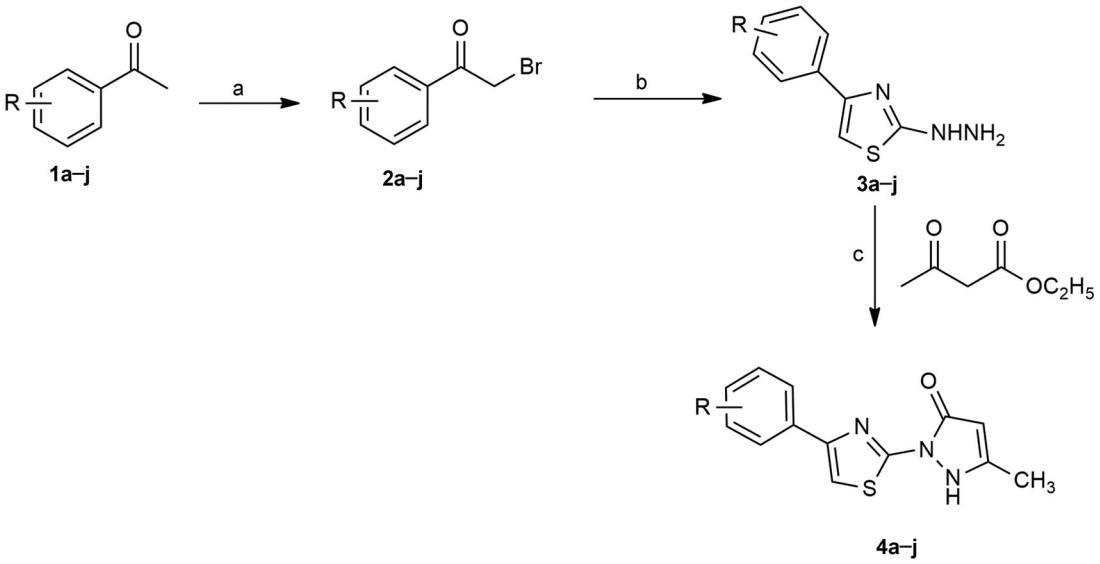

SCHEME 1 Reagents and conditions: (a) Br_2, reflux; (b) thiosemicarbazide, propane-2-ol, reflux; (c) dimethylformamide, reflux

TABLE 1 In vitro angiotensin-converting enzyme inhibition of compounds **4a–j**

Compound	Substituent	% inhibition
4a	H	43
4b	4-OH	67
4c	4-CH_3	55
4d	4-OCH_3	62
4e	4-NO_2	70
4f	4-Cl	80
4g	4-Br	76
4h	4-F	90
4i	2-Cl, 4-F	95
4j	2,4-di-Cl	84
Lisinopril		99

that is, *para*-nitro and *para*-chloro in the case of compounds **4e** and **4f**, respectively. On the contrary, the activity was decreased mildly in the case of compound **4g** having *para*-bromo. In the next instance, the percentage of inhibition was further improved significantly in the case of compounds **4h** and **4i** having *ortho*-chloro and *para*-fluoro, respectively. The last compound of the tested series showed a drop in the inhibitory activity after the introduction of chloro in the place of *para*-fluoro (84%). Among the tested series, compound **4i** was revealed as the most potent ACE inhibitor having 95% inhibitory activity, whereas none of the synthesized derivatives showed an inhibitory activity comparable to or more than lisinopril as the standard drug. The structure–activity relationship of the designed analogs suggested that the electron-withdrawing groups have a significant influence on the inhibitory activity as compared with their electron-releasing counterparts. More important, the disubstituted molecule with two distinct halogen atoms (**4i**) was found more active than the same halogen disubstituted molecule (**4j**). This suggests that the same substitution on the ring does not favor activity. Encouraged by the excellent ACE inhibitory activity of compound **4i** and the importance of ACE inhibitors in MI, it is worthwhile to determine the cardioprotective activity of compound **4i** in the isoproterenol (ISO)-induced MI in rats. The induction of MI in rats by ISO is a very popular model in determining the cardioprotective effect of any new medicinal agent. ISO chemically belongs to the class of catecholamine and possesses β-adrenergic agonistic activity. It causes severe stress in the myocardial tissue, resulting in infarct-like necrosis of the heart muscle, which renders it suitable for the induction of MI-like characteristics in rats.

Initially, the effect of compound **4i** was investigated on the serum biomarkers associated with cardiac injury (lactate dehydrogenase [LDH] and creatine kinase [CK]-MB) after induction with ISO.[28] As expected, the ISO-treated rats showed an increased level of LDH and CK-MB, which was later found to be reduced in **4i**-treated rats as compared with the ISO-treated group in dose-dependent manner (Figure 1).

The cardiac function is found to be altered after MI, and the ACE inhibitor was found effective in such conditions.[12,29] Therefore, it is worth to investigate the effect of compound **4i** on the cardiac functions of the rats. As shown in Figure 2, compound **4i** causes a significant improvement in left ventricular end-systolic pressure (LVSP) and $\pm dp/dt_{max}$; however, the infarct percentage was also found to be decreased significantly. Moreover, as presented in Table 2, compound **4i** causes significant progression in the posterior wall thickness of the LV with simultaneous augmentation in the mass of LV. The end-systolic volume was also found to be increased in the **4i**-treated group as compared with the ISO-treated group.

Oxidative stress and inflammation are the characteristic features of the MI, and various studies have shown the role of oxidative stress in the progression of inflammation in MI.[30–34] Concerning this, the effect of compound **4i** was investigated on the various biomarkers denoting the expression of oxidative stress (malondialdehyde [MDA],

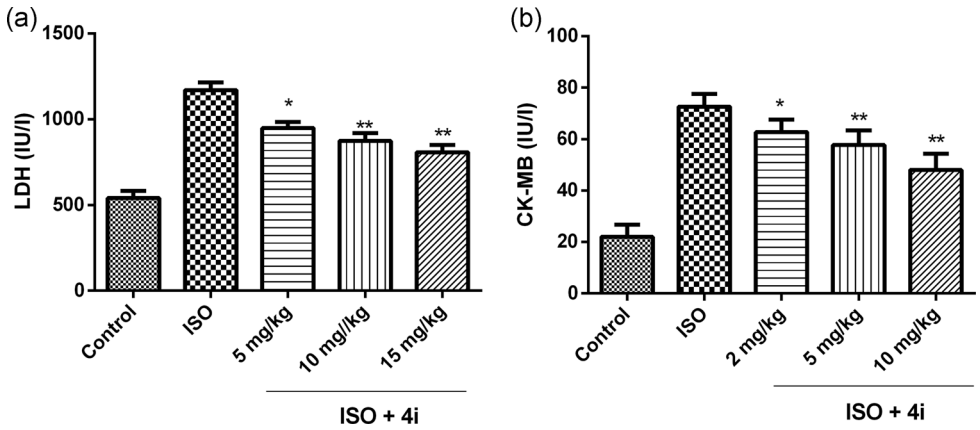

FIGURE 1 The effect of compound **4i** on serum (a) LDH and (b) CK-MB levels. Data represent the mean (±*SEM*) of three independent experiments. CK-MB, creatine kinase-MB; ISO, isoproterenol; LDH, lactate dehydrogenase; *SEM*, standard error of the mean. $^{*}p < .05$ versus ISO-treated group; $^{**}p < .01$ versus ISO group

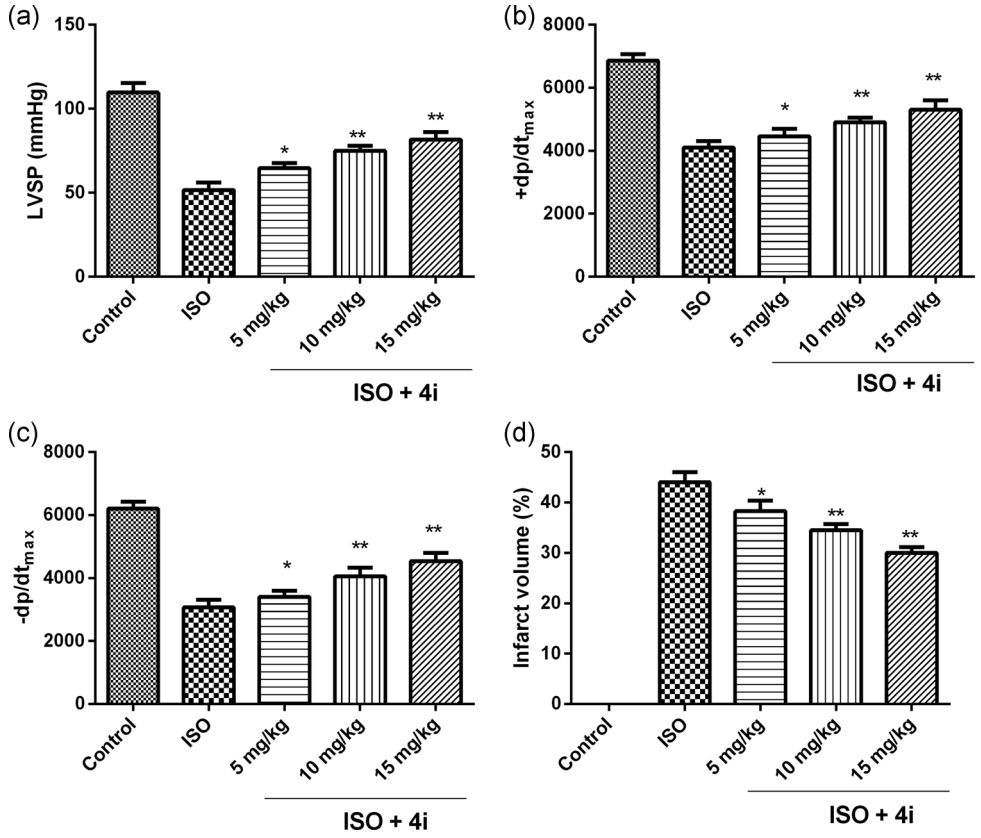

FIGURE 2 The effect of compound **4i** on (a) LVSP, (b, c) $\pm dp/dt_{max}$, and (d) infarct volume after MI. Data represent the mean (±*SEM*) of three independent experiments. ISO, isoproterenol; LVSP, left ventricular end-systolic pressure; MI, myocardial infarction; *SEM*, standard error of the mean. *$p < .05$ versus ISO-treated group; **$p < .01$ versus ISO group

myeloperoxidase [MPO], glutathione peroxidase [GPx], and superoxide dismutase [SOD]) and myocardial inflammation (Tn-T, tumor necrosis factor-α [TNF-α], and interleukin-6 [IL-6] level). It has been found that compound **4i** causes a significant reduction in oxidative stress by increasing the level of GPx and SOD, whereas the level of MPO and MDA was found to be reduced significantly as compared with the ISO-treated group in a dose-dependent manner (Figure 3a–d). As shown in Figure 3e–g, the level of various inflammatory markers (Tn-T, TNF-α, and IL-6) was reduced significantly in **4i**-treated group as compared with the ISO-treated group.

Numerous studies have shown the role of apoptosis in CVDs. It has been found that during hypoxia and ischemia/reperfusion, the cardiomyocytes undergo necrosis and initiate a cascade of events involving mitochondrial genes (Bcl-2, Bax, and caspase-3).[35–37] These genes are classified as proapoptotic (Bax) and apoptotic gene (Bcl-2), where their intricate balance controls apoptosis. Moreover, caspase-3 is another vital gene involved in the repair of DNA and membrane integrity. Therefore, the effect of compound **4i** was investigated on cardiac Bcl-2, Bax, and caspase-3 via the Western blot analysis. Results suggested that the expression of cleaved caspase-3 and Bax was found to be downregulated in the **4i**-treated group, with the upregulation of Bcl-2, as compared with the ISO-treated group (Figure 4).

TABLE 2 The effect of compound **4i** on cardiac function in rats (echo readings)

Parameters	Pre	Post
PWT (mm)	1.32 ± 0.04	1.48 ± 0.05
ESV (μl)	152 ± 8	205 ± 16
EDV (μl)	339 ± 19	406 ± 21
EF (%)	55.1 ± 3.3	49.5 ± 4.2

Abbreviations: EDV, end-diastolic volume; EF, ejection fraction; ESV, end-systolic volume; PWT, posterior wall thickness.

3 | CONCLUSION

Collectively, our study showed the development of novel thiazole–pyrazolone hybrids as potent ACE inhibitors, possessing a mild-to-significant inhibitory activity. Among the tested series, compound **4i** was found as the most potent inhibitor of ACE. The effect of compound **4i** was also investigated in isoproternol-induced MI in rats. It has been found that compound **4i** improves hemodynamic parameters with a reduction of infarct size in rats. It also causes inhibition of oxidative stress and inflammation in cardiac tissues. Compound **4i** also prevented necrosis of cardiomyocytes by inhibiting apoptosis.

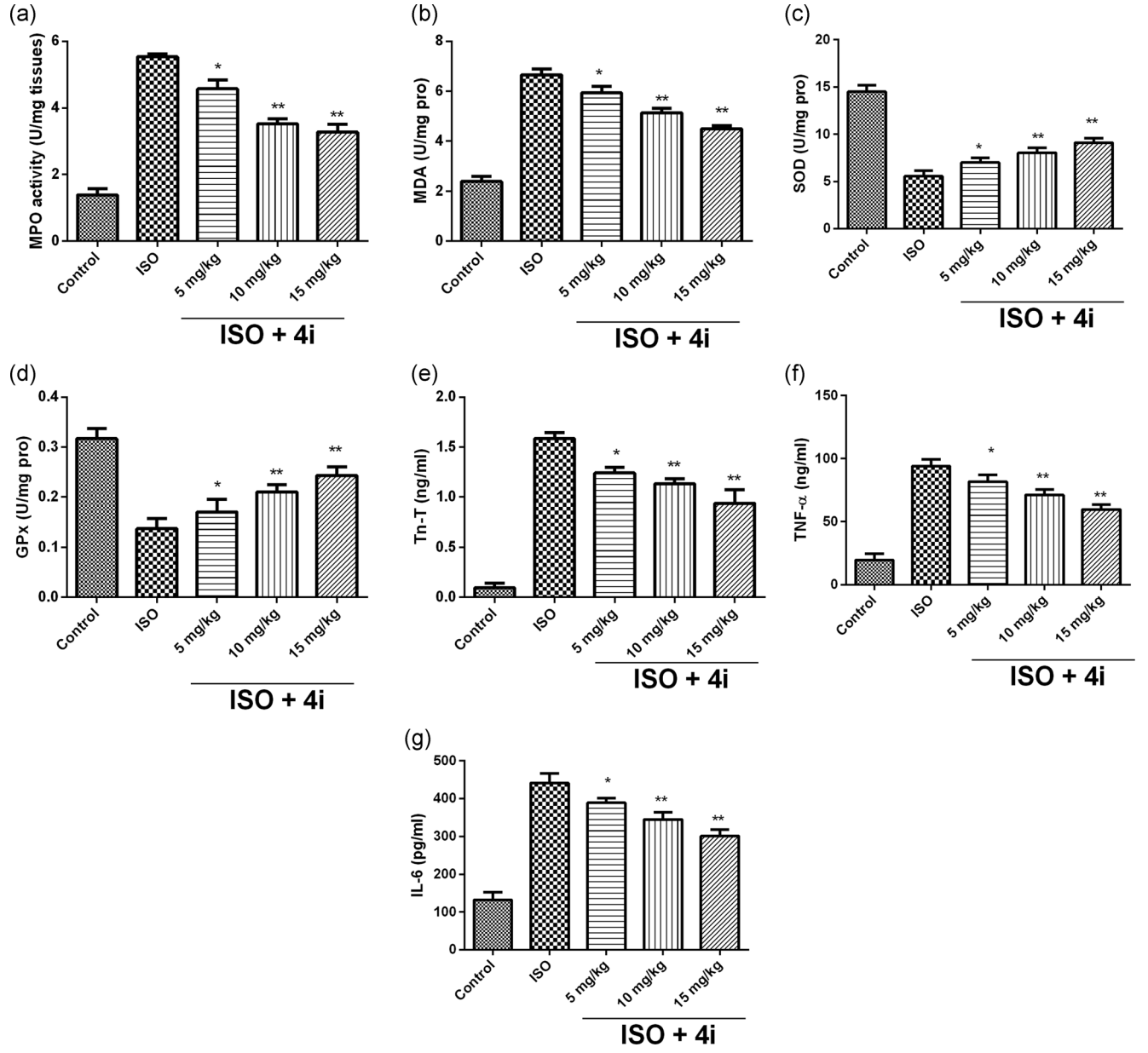

FIGURE 3 The effect of compound **4i** on the cardiac biomarkers depicting oxidative stress and inflammation: (a) MPO, (b) MDA, (c) SOD, (d) GPx, (e) Tn-T, (f) TNF-α, and (g) IL-6. Data represent the mean (±*SEM*) of three independent experiments. GPx, glutathione peroxidase; IL-6, interleukin-6; ISO, isoproterenol; MDA, malondialdehyde; MPO, myeloperoxidase; *SEM*, standard error of the mean; TNF-α, tumor necrosis factor-α. $^{*}p < .05$ versus ISO-treated group; $^{**}p < .01$ versus ISO group

However, more studies are necessary to establish the present class of the compound as a novel ACE inhibitor against MI.

4 | EXPERIMENTAL

4.1 | Chemistry

4.1.1 | General

The chemicals used in the present study were obtained from Sigma-Aldrich. NMR spectra were recorded using a Bruker Avance NMR spectrometer at 400 MHz (^{1}H) or 100 MHz (^{13}C), respectively, in dimethyl sulfoxide (DMSO)-d_6, using tetramethylsilane (TMS) as an internal standard. The multiplicity of a signal is indicated as follows: s, singlet; d, doublet; t, triplet; q, quartet; m, multiplet; br, broad; dd, doublet of doublets, and so forth. Coupling constants (*J*) are quoted in hertz and reported to the nearest 0.1 Hz. Infrared spectra were recorded as a neat thin film on a PerkinElmer Spectrum One FTIR spectrometer using Universal ATR sampling accessories. Letters in the parentheses refer to the relative absorbency as compared with the most intense peak: w, weak, <40%; m, medium, 40–75%; s, strong, >75%. Melting points (MPs) were obtained using an OptiMelt automated melting point system. MS spectra were recorded on an Agilent 1100 LC/MS.

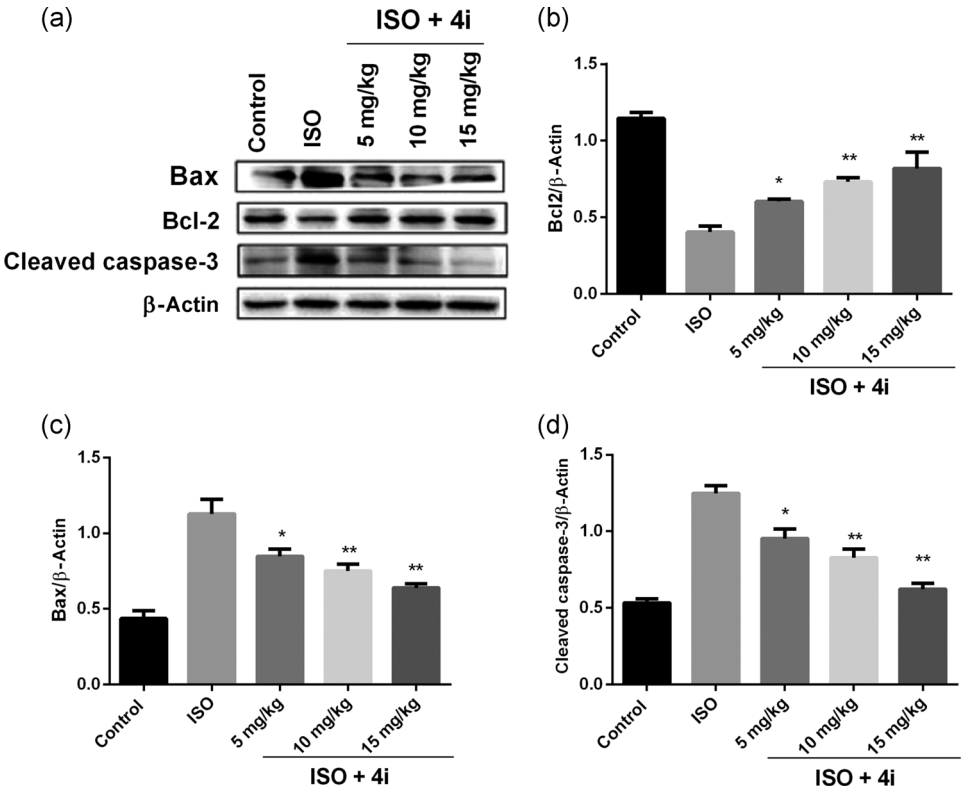

FIGURE 4 The effect of compound **4i** on (a) the Bcl-2 family proteins and a representative bar graph of (b) Bcl-2, (c) Bax, and (d) cleaved caspase-3 as determined via the Western blot analysis. Data represent the mean (±*SEM*) of three independent experiments. ISO, isoproterenol; *SEM*, standard error of the mean. *$p < .05$ versus ISO group; **$p < .01$ versus ISO-treated group

The InChI codes of the investigated compounds, together with some biological activity data, are provided as Supporting Information Data.

4.1.2 | Synthesis of compounds 2a–j and 3a–j

Compounds **2a–j** and **3a–j** were synthesized as per the earlier reported procedure.[38,39]

4.1.3 | General procedure for the synthesis of the title compounds 4a–j

A mixture of ethyl acetoacetate (5 mmol) and dimethylformamide dimethyl acetal (5.5 mmol) was refluxed to 100°C on a water bath until it changed color from yellow to orange. Then the reaction mixture was cooled to room temperature and diluted with ethanol (20 ml). The corresponding substituted thiazole derivatives **3a–j** (5 mmol) were diluted in 20 ml ethanol separately and added dropwise to the reaction mixture over 5 min. Then, it was heated to reflux for 2 hr and monitored by using thin-layer chromatography. After completion of the reaction, the reaction mixture was allowed to cool to room temperature and concentrated under reduced pressure. The resulting oil was extracted by using dichloromethane and washed with 10% sodium bicarbonate and saturated brine solution; then, the organic layer was dried over anhydrous sodium sulfate, filtered, and concentrated in vacuo. The residue was purified by recrystallization using ethanol solvent.

*5-Methyl-2-(4-phenylthiazol-2-yl)-1,2-dihydro-3*H*-pyrazol-3-one (**4a**)*

Yield: 79%; white solid; MP: 193–196°C; molecular weight (MW): 257.31; retention factor (R_f): 0.69; FTIR (ν_{max}; cm^{-1} KBr): 3,387 (N–H stretching, –NH), 3,087 (Ar C–H stretching), 2,958 (alkyl C–H stretching), 1,709 (C=O stretching), 1,682 (C=N aromatic), 1,625 (C=C stretching), 1,132 (aromatic C–C stretching), 1,508 (N–H bend, NH), 1,049 (C–N stretching), 634 (C–S stretching) cm^{-1}; ^{1}H NMR (400 MHz, DMSO-d_6, TMS) δ ppm: 7.87 (d, 2H, J = 7.6 Hz, Ar-H), 7.38 (d, 2H, J = 7.2 Hz, Ar-H), 7,34 (t, 1H, J = 1.4 Hz, Ar-H), 7.24 (s, 1H, thiazole-H), 5.65 (s, 1H, pyrazole-H), 3.98 (s, 1H, pyrazole-NH), 2.35 (s, 3H, pyrazole-CH_3); ^{13}C NMR (100 MHz, DMSO-d_6) δ ppm: 173.3, 165.9, 152.1, 150.2, 133.2, 129.4, 128.7, 127.6, 105.1, 94.2, 13.9; mass: 258.34 (M+1); elemental analysis for $C_{13}H_{11}N_3OS$: calculated: C, 60.68; H, 4.31; N, 16.33; found: C, 60.69; H, 4.35; N, 16.32.

*2-[4-(4-Hydroxyphenyl)thiazol-2-yl]-5-methyl-1,2-dihydro-3*H*-pyrazol-3-one (**4b**)*

Yield: 82%; black solid; MP: 242–243°C; MW: 273.31; R_f: 0.74; FTIR (ν_{max}; cm^{-1} KBr): 3,427 (OH stretching), 3,391 (N–H stretching, –NH),

3,082 (Ar C–H stretching), 2,959 (alkyl C–H stretching), 1,711 (C═O stretching), 1,684 (C═N aromatic), 1,626 (C═C stretching), 1,131 (aromatic C–C stretching), 1,507 (N–H bend, NH), 1,051 (C–N stretching), 639 (C–S stretching) cm^{-1}; ^1H NMR (400 MHz, DMSO-d_6, TMS) δ ppm: 9.34 (s, 1H, Ar-OH), 7.62 (d, 2H, J = 7.8 Hz, Ar-H), 7.18 (s, 1H, thiazole-H), 7.05 (d, 2H, J = 6.3 Hz, Ar-H), 5.64 (s, 1H, pyrazole-H), 3.97 (s, 1H, pyrazole-NH), 2.36 (s, 3H, pyrazole-CH_3); ^{13}C NMR (100 MHz, DMSO-d_6, TMS) δ ppm: 173.3, 165.7, 158.3, 152.2, 150.4, 128.9, 125.4, 116.5, 105.1, 94.1, 13.9; mass: 274.37 (M+1); elemental analysis for $C_{13}H_{11}N_3O_2S$: calculated: C, 57.13; H, 4.06; N, 15.37; found: C, 57.16; H, 4.05; N, 15.39.

*5-Methyl-2-[4-(p-tolyl)thiazol-2-yl]-1,2-dihydro-3H-pyrazol-3-one (**4c**)*

Yield: 76%; light yellow solid; MP: 214–216°C; MW: 271.34; R_f: 0.79; FTIR (ν_{max}; cm^{-1} KBr): 3,387 (N–H stretching, –NH), 3,084 (Ar C–H stretching), 2,952 (alkyl C–H stretching), 1,713 (C═O stretching), 1,687 (C═N aromatic), 1,621 (C═C stretching), 1,134 (aromatic C–C stretching), 1,509 (N–H bend, NH), 1,053 (C–N stretching), 639 (C–S stretching) cm^{-1}; ^1H NMR (400 MHz, DMSO-d_6, TMS) δ ppm: 7.58 (d, 2H, J = 7.9 Hz, Ar-H), 7.29 (s, 1H, thiazole-H), 7.19 (d, 2H, J = 6.7 Hz, Ar-H), 5.65 (s, 1H, pyrazole-H), 3.99 (s, 1H, pyrazole-NH), 2.34 (s, 3H, pyrazole-CH_3), 2.24 (s, 3H, Ar-CH_3); ^{13}C NMR (100 MHz, DMSO-d_6, TMS) δ ppm: 173.4, 165.7, 152.3, 150.2, 131.8, 130.1, 129.5, 125.8, 105.2, 94.1, 21.4, 13.8; mass: 272.36 (M+1); elemental analysis for $C_{14}H_{13}N_3OS$: calculated: C, 61.97; H, 4.83; N, 15.49; found: C, 61.99; H, 4.85; N, 15.52.

*2-[4-(4-Methoxyphenyl)thiazol-2-yl]-5-methyl-1,2-dihydro-3H-pyrazol-3-one (**4d**)*

Yield: 69%; yellow solid; MP: 206–208°C; MW: 287.34; R_f: 0.83; FTIR (ν_{max}; cm^{-1} KBr): 3,386 (N–H stretching, –NH), 3,085 (Ar C–H stretching), 2,954 (alkyl C–H stretching), 2,824 (OCH_3 stretching), 1,716 (C═O stretching), 1,689 (C═N aromatic), 1,623 (C═C stretching), 1,131 (aromatic C–C stretching), 1,508 (N–H bend, NH), 1,055 (C–N stretching), 637 (C–S stretching) cm^{-1}; ^1H NMR (400 MHz, DMSO-d_6, TMS) δ ppm: 7.46 (d, 2H, J = 7.5 Hz, Ar-H), 7.16 (s, 1H, thiazole-H), 7.01 (d, 2H, J = 6.3 Hz, Ar-H), 5.67 (s, 1H, pyrazole-H), 3.98 (s, 1H, pyrazole-NH), 3.82 (s, 3H, Ar-OCH_3), 2.35 (s, 3H, pyrazole-CH_3); ^{13}C NMR (100 MHz, DMSO-d_6, TMS) δ ppm: 173.3, 165.9, 160.7, 152.3, 150.3, 128.7, 125.4, 114.9, 105.2, 94.3, 55.9, 13.8; mass: 288.38 (M+1); elemental analysis for $C_{14}H_{13}N_3O_2S$: calculated: C, 58.52; H, 4.56; N, 14.62; found: C, 58.54; H, 4.58; N, 14.61.

*5-Methyl-2-[4-(4-nitrophenyl)thiazol-2-yl]-1,2-dihydro-3H-pyrazol-3-one (**4e**)*

Yield: 78%; yellow solid; MP: 253–254°C; MW: 302.31; R_f: 0.72; FTIR (ν_{max}; cm^{-1} KBr): 3,389 (N–H stretching, –NH), 3,082 (Ar C–H stretching), 2,953 (alkyl C–H stretching), 1,719 (C═O stretching), 1,685 (C═N aromatic), 1,628 (C═C stretching), 1,538 (NO_2 stretching), 1,136 (aromatic C–C stretching), 1,509 (N–H bend, NH), 1,057 (C–N stretching), 639 (C–S stretching) cm^{-1}; ^1H NMR (400 MHz, DMSO-d_6, TMS) δ ppm: 7.58 (d, 2H, J = 7.2 Hz, Ar-H), 7.48 (d, 2H, J = 6.1 Hz, Ar-H), 7.17 (s, 1H, thiazole-H), 5.64 (s, 1H, pyrazole-H), 3.97 (s, 1H, pyrazole-NH), 2.37 (s, 3H, pyrazole-CH_3); ^{13}C NMR (100 MHz, DMSO-d_6, TMS) δ ppm: 173.4, 165.9, 152.3, 150.2, 147.8, 139.2, 126.3, 124.5, 105.2, 94.3, 13.9; mass: 303.34 (M+1); elemental analysis for $C_{13}H_{10}N_4O_3S$: calculated: C, 51.65; H, 3.33; N, 18.53; found: C, 51.67; H, 3.38; N, 18.51.

*2-[4-(4-Chlorophenyl)thiazol-2-yl]-5-methyl-1,2-dihydro-3H-pyrazol-3-one (**4f**)*

Yield: 71%; white solid; MP: 192–194°C; MW: 291.75; R_f: 0.67; FTIR (ν_{max}; cm^{-1} KBr): 3,386 (N–H stretching, –NH), 3,084 (Ar C–H stretching), 2,958 (alkyl C–H stretching), 1,714 (C═O stretching), 1,682 (C═N aromatic), 1,629 (C═C stretching), 1,139 (aromatic C–C stretching), 1,504 (N–H bend, NH), 1,059 (C–N stretching), 787 (C–Cl stretching), 638 (C–S stretching) cm^{-1}; ^1H NMR (400 MHz, DMSO-d_6, TMS) δ ppm: 7.75 (d, 2H, J = 7.5 Hz, Ar-H), 7.59 (d, 2H, J = 6.4 Hz, Ar-H), 7.35 (s, 1H, thiazole-H), 5.65 (s, 1H, pyrazole-H), 3.96 (s, 1H, pyrazole-NH), 2.36 (s, 3H, pyrazole-CH_3); ^{13}C NMR (400 MHz, DMSO-d_6, TMS) δ ppm: 173.5, 165.9, 152.3, 150.3, 134.4, 131.2, 129.6, 128.9, 105.2, 94.4, 13.9; mass: 292.78 (M+1); elemental analysis for $C_{13}H_{10}ClN_3OS$: calculated: C, 53.52; H, 3.45; N, 14.40; found: C, 53.54; H, 3.48; N, 14.42.

*2-[4-(4-Bromophenyl)thiazol-2-yl]-5-methyl-1,2-dihydro-3H-pyrazol-3-one (**4g**)*

Yield: 77%; brownish black solid; MP: 206–209°C; MW: 336.21; R_f: 0.73; FTIR (ν_{max}; cm^{-1} KBr): 3,389 (N–H stretching, –NH), 3,081 (Ar C–H stretching), 2,959 (alkyl C–H stretching), 1,718 (C═O stretching), 1,685 (C═N aromatic), 1,628 (C═C stretching), 1,132 (aromatic C–C stretching), 1,507 (N–H bend, NH), 1,052 (C–N stretching), 758 (C–Br stretching), 635 (C–S stretching) cm^{-1}; ^1H NMR (400 MHz, DMSO-d_6, TMS) δ ppm: 7.64 (d, 2H, J = 7.8 Hz, Ar-H), 7.56 (d, 2H, J = 6.2 Hz, Ar-H), 7.30 (s, 1H, thiazole-H), 5.67 (s, 1H, pyrazole-H), 3.99 (s, 1H, pyrazole-NH), 2.34 (s, 3H, pyrazole-CH_3); ^{13}C NMR (100 MHz, DMSO-d_6, TMS) δ ppm: 173.5, 165.9, 152.3, 150.3, 132.3, 132.1, 128.4, 123.2, 105.1, 94.2, 13.8; mass: 337.24 (M+1); elemental analysis for $C_{13}H_{10}BrN_3OS$: calculated: C, 46.44; H, 3.00; N, 12.50; found: C, 46.48; H, 3.02; N, 12.52.

*2-[4-(4-Fluorophenyl)thiazol-2-yl]-5-methyl-1,2-dihydro-3H-pyrazol-3-one (**4h**)*

Yield: 73%; brown solid; MP: 251–252°C; MW: 275.30; R_f: 0.85; FTIR (ν_{max}; cm^{-1} KBr): 3,385 (N–H stretching, –NH), 3,083 (Ar C–H stretching), 2,952 (alkyl C–H stretching), 1,714 (C═O stretching), 1,687 (C═N aromatic), 1,629 (C═C stretching), 1,156 (C–F stretching), 1,136 (aromatic C–C stretching), 1,509 (N–H bend, NH), 1,053 (C–N stretching), 637 (C–S stretching) cm^{-1}; ^1H NMR (400 MHz, DMSO-d_6, TMS) δ ppm: 7.59 (d, 2H, J = 7.4 Hz, Ar-H), 7.24 (s, 1H, thiazole-H), 7.16 (d, 2H, J = 6.3 Hz, Ar-H), 5.66 (s, 1H, pyrazole-H), 3.96 (s, 1H, pyrazole-NH), 2.36 (s, 3H, pyrazole-CH_3); ^{13}C NMR (100 MHz, DMSO-d_6, TMS) δ ppm: 173.5, 165.9, 162.7, 152.3, 150.3, 130.8, 128.7, 116.1, 105.2, 94.2, 13.8; mass: 276.32 (M+1); elemental

analysis for $C_{13}H_{10}FN_3OS$: calculated: C, 56.72; H, 3.66; N, 15.26; found: C, 56.71; H, 3.64; N, 15.28.

*2-[4-(2-Chloro-4-fluorophenyl)thiazol-2-yl]-5-methyl-1,2-dihydro-3H-pyrazol-3-one (**4i**)*

Yield: 79%; red brown solid, MP: 319–320°C; MW: 309.74; R_f: 0.81; FTIR (ν_{max}; cm^{-1} KBr): 3,388 (N–H stretching, –NH), 3,082 (Ar C–H stretching), 2,956 (alkyl C–H stretching), 1,718 (C═O stretching), 1,689 (C═N aromatic), 1,623 (C═C stretching), 1,157 (C–F stretching), 1,138 (aromatic C–C stretching), 1,507 (N–H bend, NH), 1,052 (C–N stretching), 789 (C–Cl stretching), 639 (C–S stretching) cm^{-1}; ^1H NMR (400 MHz, DMSO-d_6, TMS) δ ppm: 7.86 (d, 1H, J = 7.9 Hz, Ar-H), 7.43 (d, 1H, J = 6.1 Hz, Ar-H), 7.37 (s, 1H, thiazole-H), 7.07 (d, 1H, J = 1.5 Hz, Ar-H), 5.64 (s, 1H, pyrazole-H), 3.99 (s, 1H, pyrazole-NH), 2.35 (s, 3H, pyrazole-CH_3); ^{13}C NMR (100 MHz, DMSO-d_6, TMS) δ ppm: 173.4, 165.9, 164.5, 152.2, 147.9, 133.9, 130.5, 125.6, 118.4, 114.2, 105.1, 94.1, 13.7; mass: 310.76 (M+1); elemental analysis for $C_{13}H_9ClFN_3OS$: calculated: C, 50.41; H, 2.93; N, 13.57; found: C, 50.43; H, 2.91; N, 13.59.

*2-[4-(2,4-Dichlorophenyl)thiazol-2-yl]-5-methyl-1,2-dihydro-3H-pyrazol-3-one (**4j**)*

Yield: 73%; white solid, MP: 356–357°C; MW: 326.20; R_f: 0.77; FTIR (ν_{max}; cm^{-1} KBr): 3,389 (N–H stretching, –NH), 3,085 (Ar C–H stretching), 2,959 (alkyl C–H stretching), 1,717 (C═O stretching), 1,684 (C═N aromatic), 1,626 (C═C stretching), 1,139 (aromatic C–C stretching), 1,508 (N–H bend, NH), 1,056 (C–N stretching), 787 (C–Cl stretching), 638 (C–S stretching) cm^{-1}; ^1H NMR (400 MHz, DMSO-d_6, TMS) δ ppm: 7.87 (d, 1H, J = 7.8 Hz, Ar-H), 7.67 (d, 1H, J = 6.5 Hz, Ar-H), 7.41 (s, 1H, thiazole-H), 7.32 (d, 1H, J = 1.8 Hz, Ar-H), 5.67 (s, 1H, pyrazole-H), 3.98 (s, 1H, pyrazole-NH), 2.34 (s, 3H, pyrazole-CH_3); ^{13}C NMR (100 MHz, DMSO-d_6, TMS) δ ppm: 173.4, 165.9, 152.3, 147.9, 135.9, 133.6, 130.9, 130.1, 128.2, 127.4, 105.2, 94.1, 13.8; mass: 327.24 (M+1); elemental analysis for $C_{13}H_9Cl_2N_3OS$: calculated: C, 47.87; H, 2.78; N, 12.88; found: C, 47.89; H, 2.76; N, 12.89.

4.2 | In vitro ACE inhibition study

In vitro ACE inhibition assay was performed using the colorimetric method, where 10 ml of 0.05 M sodium borate buffer, pH 8.2, containing 0.3 M NaCl and 0.5% Triton X-100, was used to suspend 1 g Rabbit Lung Acetone Powder (Sigma-Aldrich), a source of ACE enzyme, at 4°C for 24 hr, followed by centrifugation at 15,000 rpm for 60 min at 4°C. The resultant supernatant was used as a source of ACE enzyme for this assay. The release of hippuric acid (HA) resulting from the hydrolysis of the substrate hippuryl-histidyl-leucine (HHL; Sigma-Aldrich) directly correlated with the inhibitory activity of the compound. The test and standard drug lisinopril was made in a solution at 1-mM concentration and was preincubated with 7 ml of the ACE enzyme for 10 min at 37°C. The final volume was adjusted using 0.05 M sodium borate buffer (pH 8.2) containing 0.3 M NaCl to obtain identical concentration. Furthermore, the enzyme reaction was then initiated by adding 50 ml of 5 mM substrate (HHL), followed by incubation at 37°C for 30 min. The reaction was then terminated by the addition of 0.1 ml of 1 M HCl, and HA thus produced in the reaction was then allowed to react with 0.2 ml of pyridine and 0.1 ml of benzene sulfonyl chloride (Sigma-Aldrich) to develop yellow color. This specific color was measured at 410 nm. The ACE inhibition was expressed as percentage inhibition and calculated from the following equation: Inhibition% = 100 − [T/C] × 100, where T is the absorbance of test reaction and C is the absorbance of control reaction. The therapeutic drug lisinopril was used as a reference ACE inhibitor.

4.2.1 | Animals

After obtaining from the institutional animal house, the adult male Sprague Dawley (240–270 g) rats were housed under controlled temperature and humidity. The rats were acclimatized to the laboratory environment via exposing them to alternate, dark and light cycle with ad libitum supply of food and water.

4.2.2 | Ethics statement

The experimental procedures involving animals in this study were approved by the Animal Ethics Committee of the Institute and Experimental Animal Regulation by the National Science and Technology Commission, China, for the use of laboratory animals.

4.2.3 | Initiation of experimental MI

Experimental MI was induced via subcutaneous injection of ISO in rats after dissolving in normal saline (100 mg/kg) at a period of 24 hr for 2 days.

4.2.4 | Experimental design

The animals were randomly divided into five groups (12 rats each).

Group 1: normal control; Group 2: ISO rats; Group 3: compound **4i** (5 mg/kg) + ISO; Group 4: compound **4i** (10 mg/kg) + ISO; Group 5: compound **4i** (15 mg/kg) + ISO. Compound **4i** after suspending in 0.5% carboxymethyl cellulose was orally administered once a day to rats for the duration of 10 days (once a day) using an intragastric tube. The rats were killed to isolate serum and plasma by cervical decapitation after 12 hr of the second dose of ISO. The heart tissues were isolated and washed in chilled normal saline. The supernatant obtained after homogenization of heart tissues in Tris-HCl buffer (pH 7.4) was used for the estimation of various biochemical parameters.

4.2.5 | Evaluation of hemodynamic parameters

After the first ISO injection, the blood pressure and heart rate were taken at 48 hr using a computerized, noninvasive tail-cuff system,

Visitech BP-2000 Blood Pressure Analysis System™ (Visitech Systems, Apex, NC, USA). Thereafter, all the rats were anesthetized with urethane to measure the left ventricular function. The LVSP, left ventricular end-diastolic pressure, and left ventricular maximum rate of positive or negative pressure development ($\pm LVdp/dt_{max}$) were recorded using a BL-420E monitor system (Chengdu, China).

4.2.6 | Infarct size measurement

For infarct size measurement, rats from different groups were carefully dissected and 2-mm-thick sections were sliced. The infarct size of rats was determined with 5-triphenyltetrazolium chloride (Sigma-Aldrich Co.) at 37°C for 30 min in the dark. The region of the heart with no color was supposed as the ischemic heart muscles, whereas the area with brick red color was deemed as regular myocardium. The area of infarct size was recorded by the volume and weight as a percentage of the left ventricle.

4.2.7 | Enzyme-linked immunosorbent assay of LDH, CK-MB, cTn-T, TNF-α, and IL-6

Immediately, blood samples were centrifuged at 12,000*g* for 10 min at 4°C, and then the supernatant was collected for measurement at −20°C. Activities of LDH, CK-MB, Tn-T, TNF-α, and IL-6 were performed using a suite of commercial kits in accordance with the manufacturer's instructions (Beyotime Institute of Biotechnology, Nanjing, China).

4.2.8 | Determination of the level of MDA, SOD, GPx, and MPO activities

The level of MDA, SOD, GPx, and MPO activities in myocardial tissues was calculated using kits in accordance with the protocol supplied by the manufacturers.

4.2.9 | Echocardiography

The echocardiography (echo) was performed at the beginning of the experiment and on the day of sacrifice to estimate the outcome on cardiovascular function and its morphology.

4.2.10 | Western blot analysis

Total proteins were extracted from myocardial tissues using ice-cold radioimmunoprecipitation assay lysis buffer. Dissolved proteins were collected and centrifuged at 12,000 rpm for 5 min at 4°C. The bicinchoninic acid protein assay reagent was used to estimate the concentration of total protein. Isolated proteins were loaded on sodium dodecyl sulfate-polyacrylamide gel electrophoresis and shifted to the polyvinylidene fluoride membrane, and probed with primary antibodies (1:1,000 in 1% bovine serum albumin [BSA]/TBS-T) overnight at 4°C. The membranes were then washed twice for 15 min each in TBS-T and incubated with horseradish peroxidase-conjugated goat anti-mouse or rabbit antibodies (1:10,000 in 1% BSA/TBS-T).

4.2.11 | Statistical analysis

Data were analyzed by SPSS 17.0 software and expressed as the mean ± standard error of the mean. Differences were analyzed by one-way analysis of variance, followed by Dunnett's test for individual comparisons between each group mean. A *p*-value of .05 was considered statistically significant.

CONFLICTS OF INTERESTS

The authors declare that there are no conflicts of interests.

DATA AVAILABILITY STATEMENT

The data that support the findings of this study are available from the corresponding author upon reasonable request.

ORCID

Guoying Su http://orcid.org/0000-0002-4462-2587

REFERENCES

[1] D. S. Moodie, *Congenit. Heart Dis.* **2016**, *11*, 213.
[2] V. L. Roger, *Med. Clin. North Am.* **2007**, *91*, 537.
[3] S. S. Hu, L. Z. Kong, R. L. Gao, M. L. Zhu, W. Wang, Y. J. Wang, Z. S. Wu, W. W. Chen, M. B. Liu, Editorial Board, *Biomed. Environ. Sci.* **2012**, *25*, 251.
[4] Y. Bei, C. Shi, Z. Zhang, J. Xiao, *J. Cardiovasc. Transl. Res.* **2019**, *12*, 165.
[5] H. D. White, D. P. Chew, *Lancet* **2008**, *372*, 570.
[6] E. Boersma, N. Mercado, D. Poldermans, M. Gardien, J. Vos, M. L. Simoons, *Lancet* **2003**, *361*, 847.
[7] J. L. Izzo, M. R. Weir, *J. Clin. Hypertens.* **2011**, *13*, 667.
[8] D. Coates, *Int. J. Biochem. Cell Biol.* **2003**, *35*, 769.
[9] S. Heeneman, J. C. Sluimer, M. J. A. P. Daemen, *Circ. Res.* **2007**, *101*, 441.
[10] D. W. Cushman, M. A. Ondetti, *Nat. Med.* **1999**, *5*, 1110.
[11] R. W. Piepho, *Am. J. Health Syst. Pharm* **2000**, *57*, S3.
[12] M. A. Crackower, R. Sarao, G. Y. Oudit, C. Yagil, I. Kozieradzki, S. E. Scanga, A. J. Oliveira-dos-Santos, J. da Costa, L. Zhang, Y. Pei, J. Scholey, C. M. Ferrario, A. S. Manoukian, M. C. Chappell, P. H. Backx, Y. Yagil, J. M. Penninger, *Nature* **2002**, *417*, 822.
[13] H. Eckert, *Molecules* **2012**, *17*, 1074.
[14] A. Tanitame, Y. Oyamada, K. Ofuji, M. Fujimoto, N. Iwai, Y. Hiyama, K. Suzuki, H. Ito, H. Terauchi, M. Kawasaki, K. Nagai, M. Wachi, J. Yamagishi, *J. Med. Chem.* **2004**, *47*, 3693.
[15] M. F. El Shehry, M. M. Ghorab, S. Y. Abbas, E. A. Fayed, S. A. Shedid, Y. A. Ammar, *Eur. J. Med. Chem.* **2018**, *143*, 1463.
[16] B. Singh, H. R. Bhat, M. K. Kumawat, U. P. Singh, *Bioorg. Med. Chem. Lett.* **2014**, *24*, 3321.
[17] S. Y. Hassan, *Molecules* **2013**, *18*, 2683.
[18] J. Wu, J. Wang, D. Hu, M. He, L. Jin, B. Song, *Chem. Cent. J.* **2012**, *6*, 51. https://doi.org/10.1186/1752-153X-6-51

[19] J. Sun, Y. Zhou, *Molecules* **2015**, *20*, 4383.
[20] S. R. Shih, T. Y. Chu, G. R. Reddy, S. N. Tseng, H. L. Chen, W. F. Tang, M. S. Wu, J. Y. Yeh, Y. S. Chao, J. T. Hsu, H. P. Hsieh, J. T. Horng, *J. Biomed. Sci.* **2010**, *17*, 13.
[21] B. D. Cox, A. R. Prosser, Y. Sun, Z. Li, S. Lee, M. B. Huang, V. C. Bond, J. P. Snyder, M. Krystal, L. J. Wilson, D. C. Liotta, *ACS Med. Chem. Lett.* **2015**, *6*, 753.
[22] C. E. Mowbray, C. Burt, R. Corbau, S. Gayton, M. Hawes, M. Perros, I. Tran, D. A. Price, F. J. Quinton, M. D. Selby, P. A. Stupple, R. Webster, A. Wood, *Bioorg. Med. Chem. Lett.* **2009**, *19*, 5857.
[23] U. Sankappa Rai, A. M. Isloor, P. Shetty, K. S. R. Pai, H. K. Fun, *Arab. J. Chem.* **2015**, *8*, 317.
[24] B. P. Bandgar, J. V. Totre, S. S. Gawande, C. N. Khobragade, S. C. Warangkar, P. D. Kadam, *Bioorg. Med. Chem.* **2010**, *18*, 6149.
[25] C. B. Mishra, S. Kumari, M. Tiwari, *Eur. J. Med. Chem.* **2015**, *92*, 1.
[26] C. Jiang, Z. Yuan, J. F. Wang, H. Liu, J. Sun, D. Pu, W. Xia, *Lat. Am. J. Pharm.* **2016**, *35*, 440.
[27] G. Nalajam, R. R. Vedula, *J. Chem. Res.* **2008**, *1*, 195.
[28] D. W. Kehl, N. Iqbal, A. Fard, B. A. Kipper, A. De La Parra Landa, A. S. Maisel, *Transl. Res.* **2012**, *159*, 252.
[29] R. T. Tsuyuki, M. Fradette, J. A. Johnson, T. J. Bungard, D. T. Eurich, T. Ashton, W. Gordon, R. Ikuta, J. Kornder, E. Mackay, D. Manyari, K. O'Reilly, W. Semchuk, *J. Card. Failure* **2004**, *10*, 473.
[30] R. Gill, A. Tsung, T. Billiar, *Free Radical Biol. Med.* **2010**, *48*, 1121.
[31] K. Husain, *World J. Biol. Chem.* **2015**, *6*, 209.
[32] F. Bonomini, S. Tengattini, A. Fabiano, R. Bianchi, R. Rezzani, *Histol. Histopathol.* **2008**, *23*, 381.
[33] C. Di Filippo, S. Cuzzocrea, F. Rossi, R. Marfella, M. D'Amico, *Cardiovasc. Drug Rev.* **2006**, *24*, 77.
[34] F. J. Pashkow, *Int. J. Inflammation* **2011**, *2011*, 1.
[35] P. A. Krijnen, R. Nijmeijer, C. J. Meijer, C. A. Visser, C. E. Hack, H. W. Niessen, *J. Clin. Pathol.* **2002**, *55*, 801.
[36] M. T. Crow, K. Mani, Y. J. Nam, R. N. Kitsis, *Circ. Res.* **2004**, *95*, 957.
[37] Y. Lee, Å. B. Gustafsson, *Apoptosis* **2009**, *14*, 536.
[38] J. Dimmock, J. McColl, S. Wonko, R. Thayer, D. Hancock, *Eur. J. Med. Chem.* **1991**, *26*, 529.
[39] U. P. Singh, R. K. Singh, H. R. Bhat, Y. P. Subhashchandra, V. Kumar, M. K. Kumawat, P. Gahtori, *Med. Chem. Res.* **2011**, *20*, 1603.

SUPPORTING INFORMATION

Additional supporting information may be found online in the Supporting Information section.

How to cite this article: You H, Su X, Su G. Novel thiazole–pyrazolone hybrids as potent ACE inhibitors and their cardioprotective effect on isoproterenol-induced myocardial infarction. *Arch Pharm.* 2020;e2000140. https://doi.org/10.1002/ardp.202000140